

Identification of near-fault velocity pulses and prediction of resulting response spectra

Jack W. Baker¹, M. ASCE

¹Assistant Professor, Dept. of Civil and Environmental Eng.; Terman Engineering Center #240, Stanford University, Stanford, CA 94304; bakerjw@stanford.edu

ABSTRACT: Pulse-like near-fault ground motions resulting from directivity effects are a special class of ground motions that are challenging to characterize for seismic performance assessment. These motions contain a pulse in the velocity time history of the motion, often occurring in the direction perpendicular to the fault rupture at locations near the fault where the earthquake rupture has propagated towards the site. A recently proposed wavelet-based signal processing approach is used on a large ground motion library to empirically identify these pulses in ground motions. Example results are presented to demonstrate that the identified motions are often observed at sites where directivity effects are expected (although no claim is made that all observed pulses are due to directivity). The response spectra of these records are then studied using this approach, and it is seen that their spectra can be described using an existing ground motion prediction (attenuation) model coupled with a narrow-band amplification function in the region of the pulse period. The modified prediction can be incorporated in probabilistic seismic hazard analysis, providing a direct and transparent method of accounting for directivity effects.

INTRODUCTION

Pulse-like near-fault ground motions resulting from directivity effects are a special class of ground motions that are particularly challenging to characterize for seismic performance assessment. These motions contain a ‘pulse’ in the velocity time history of the motion, ideally in the direction perpendicular to the fault rupture, and generally occurring at locations near the fault where the earthquake rupture has propagated towards the site (see examples in Figure 1). Despite our growing understanding of these ground motions, it is still difficult to identify this effect and account for it in ground motion prediction (attenuation) models.

The author recently proposed a ground motion processing that allows for automated detection of directivity pulses (Baker 2007). That detection scheme is here used on a large ground motion library to empirically identify those records containing pulses. Those records are then analyzed to determine the effect of the pulses on resulting response spectra. This analysis is needed to for so-called narrow-band predictions of response spectra from near-fault ground motions, which can then be incorporated into a generalization of probabilistic seismic hazard analysis that accounts for directivity

effects (Tothong et al. 2007). Taken with other parallel developments, this work helps point the way towards a comprehensive framework to understand and account for directivity effects in engineering design. The benefits of such an approach are improved understanding of the impact that directivity has on seismic hazard, a more transparent method of accounting for these effects, and a potential reduction in conservatism associated with using “worst case” directivity scenarios for design.

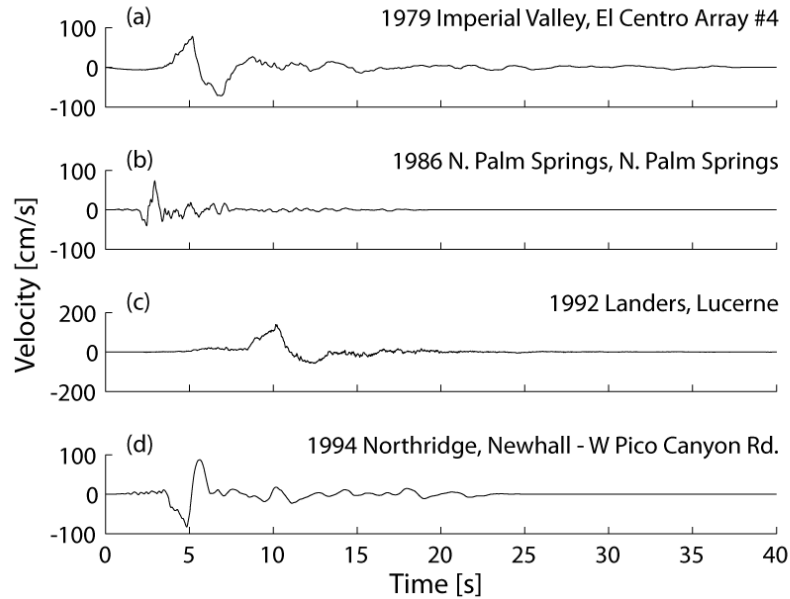


Figure 1: Four example pulse-like near-fault ground motions.

PULSE IDENTIFICATION AND EXTRACTION

The pulse extraction procedure used here relies on wavelet analysis to identify large pulses in the velocity time history of a ground motion (e.g., Mallat 1999). The wavelet transform is analogous to a Fourier transform, except that non-stationary functions are used for the decomposition instead of continuous sine functions in the case of the Fourier transform. A variety of “mother wavelets” can be used for the analysis; this mother wavelet is scaled (dilated) and translated to represent various components of the signal. A wavelet basis function is thus defined as

$$\Phi_{s,l}(t) = \frac{1}{\sqrt{s}} \Phi\left(\frac{t-l}{s}\right) \quad (1)$$

where $\Phi(\cdot)$ is the mother wavelet function, s is the scale parameter that dilates the wavelet, and l is the location parameter that translates the wavelet in time. The ground motion of interest is then transformed into coefficients for these wavelet functions with varying scale and location. There are two types of wavelet transforms available to analysts. Loosely speaking, the *discrete wavelet transform* computes only coefficients for the minimum number of wavelet basis functions needed to reconstruct a signal, while the *continuous wavelet transform* computes coefficients for every

possible scale and location. Here the continuous transform is used, as it will precisely identify the scale and location of large velocity pulses of interest.

The utility of this signal processing procedure is that if the wavelet basis function is similar in shape to velocity pulses caused by directivity, then the velocity pulse will show up in the wavelet transform as a large coefficient for the wavelet having a scale and location associated with the pulse. That wavelet coefficient can be used to both detect the presence of a pulse, as well as to extract the pulse from the ground motion.

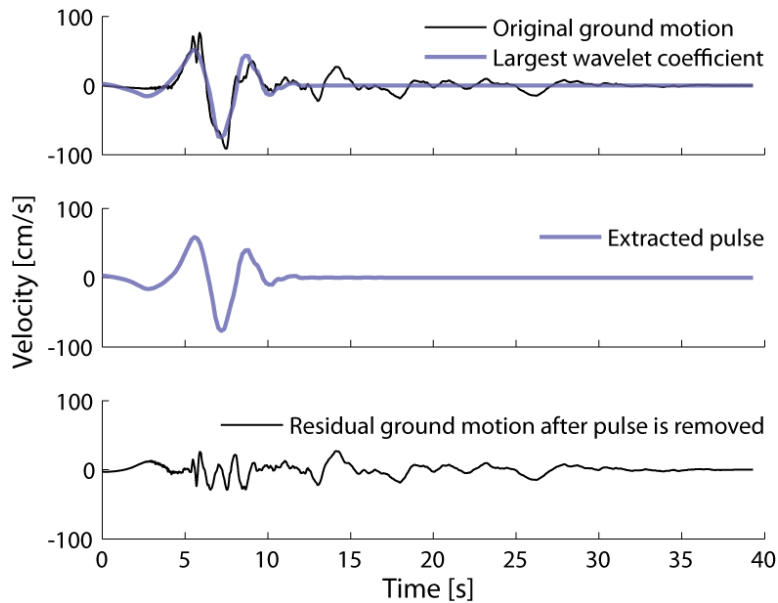


Figure 2: Illustration of the decomposition procedure used to extract the pulse portion of the 1979 Imperial Valley El Centro Array #5 recording.

Results from this algorithm are shown in Figure 2. The continuous wavelet transform is performed on the original ground motion, and the largest wavelet coefficient is identified. That wavelet, which represents the largest velocity pulse in the signal, is then refined by adding up to nine additional wavelets having the same dominant frequency and located in the region of the original wavelet. The refined pulse is then subtracted from the original ground motion, leaving a residual ground motion that contains all information not included in the pulse. Pulses are identified by comparing the peak ground velocity and energy of the residual ground motion relative to the original ground motion. This wavelet-based extraction procedure is the most important part of the pulse-identification approach, but two additional criteria were proposed as potentially useful supplemental tests. First, ground motions with a peak ground velocity of less than 30 cm/s were excluded from consideration, as the low peak velocity would suggest that even if a pulse-like feature is present in a given ground motion, the low ground motion amplitude suggests that the feature may not be caused by directivity. Second, a criterion was applied to ensure that the velocity pulse appears early in the strong ground shaking, where a directivity pulse is expected to occur. Complete details of this algorithm, which has been described only schematically here, are given by Baker (2007).

OBSERVATIONS FROM PAST EARTHQUAKES

One benefit of this analysis procedure is that large numbers of ground motions can be processed. The algorithm requires only a few seconds on a desktop computer to analyze a typical ground motion (consisting of several thousand discrete velocity values), so the approximately 3500 fault-normal ground motions from the Next Generation Attenuation (NGA) project were analyzed, and 91 pulse-like ground motions were detected. It should be noted that not all of these pulses are necessarily caused by directivity effects, although individual study of the records suggests that at least a majority are. (In particular, long-period record processing can make a static displacement due to fling effects look like a directivity pulse.) Because this procedure is at present the only way to automatically classify large numbers of ground motions, it has been implemented in the Pacific Earthquake Engineering Research (PEER) center's Design Ground Motion Library (DGML).

Having this large set of classified ground motions allows for several new ways to study pulses. Figure 3 shows maps of locations with ground motion recordings in past earthquakes, with the style of the points indicating the classification of that particular recording. It can be seen that pulses are generally observed at locations close to the fault where the rupture propagated towards the site. It is also interesting to note that at some sites very close to the faults, no pulse is observed, indicating that even at locations where directivity effects are likely, they are not certain to occur. Iervolino and Cornell (2007) have used regression analysis on this dataset to develop predicted probabilities of occurrence of pulses, as a function of several predictor variables relating to source/site geometry.

The period of an extracted velocity pulse can be defined as the period for which the Fourier spectrum of the pulse's wavelet is maximized. Many authors have noted a dependence of pulse period on the magnitude of the causal earthquake, and that trend was also confirmed using this dataset (e.g., Bray and Rodríguez-Marek 2004; Mavroeidis and Papageorgiou 2003; Somerville 2003). Baker (2007) obtained the following predictive relationship for pulse period

$$E[\ln T_p] = -5.78 + 1.02M \quad (2)$$

where T_p is the period of the pulse (as determined using wavelet analysis), $E[\]$ denotes an expected (mean) value, and M is the earthquake's moment magnitude. The standard deviation of observed $\ln T_p$ values about this mean prediction is 0.55.

RESPONSE SPECTRA OF PULSE-LIKE MOTIONS

The effect of near-fault directivity on observed response spectra was first studied systematically by Somerville et al. (1997), who predicted a broad-band modification to amplify all spectral values monotonically as a function of source/site geometry parameters that suggest directivity effects might be present. But a more accurate model would amplify spectral accelerations only in a narrow band around the pulse period. (Alavi and Krawinkler 2001; Fu and Menun 2004; Somerville 2003; Tothong

and Cornell 2007).

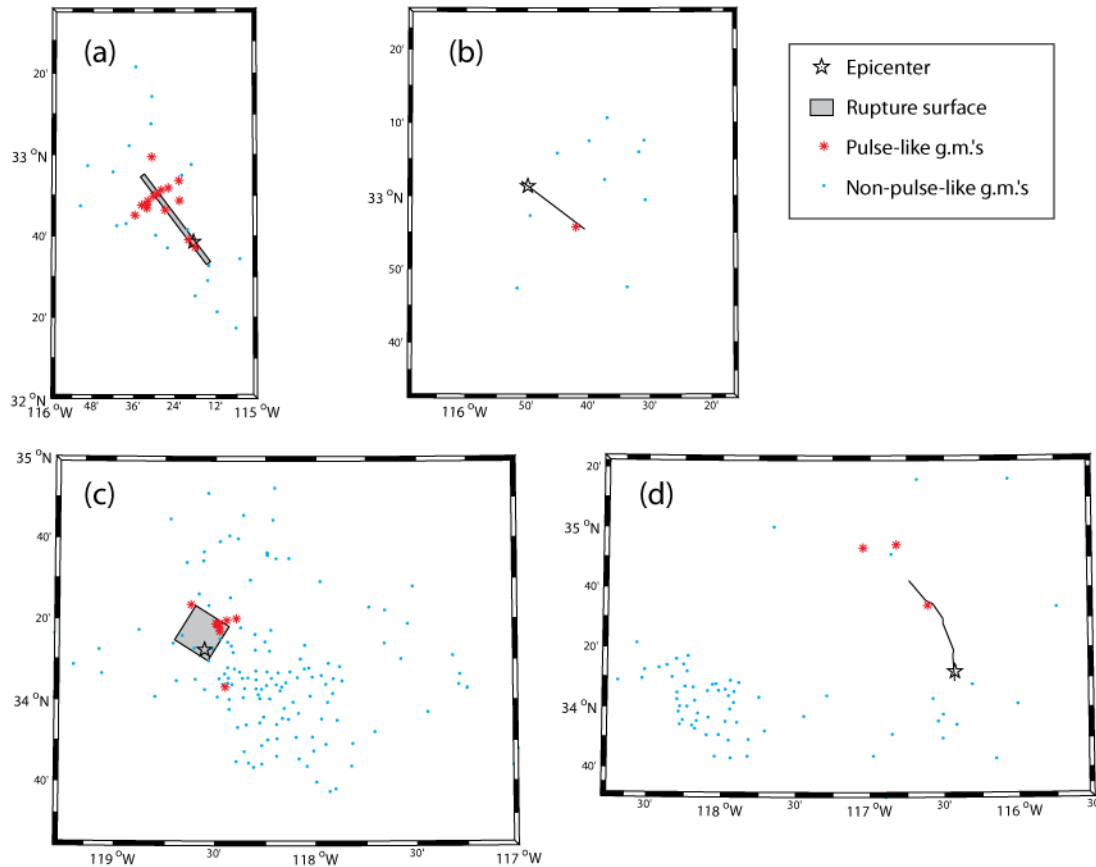


Figure 3: Maps of rupture projection and observed ground motions from four example earthquakes: (a) 1979 Imperial Valley, (b) 1987 Superstition Hills, (c) 1994 Northridge, (d) 1992 Landers.

The wavelet decomposition described above greatly facilitates quantification of the effect of the pulse on the response spectrum. In Figure 4, (pseudo) acceleration spectra of four pulse-like motions are shown, along with spectra of the motions after the pulses have been extracted. Median predicted spectra (Boore and Atkinson 2007) are also shown, as well as marks indicating the motions' pulse periods. It is apparent that the pulses cause amplification of the records' spectra, in the region of the pulse period. These amplification regions are shaded in Figure 4 for emphasis.

To more systematically quantify this amplification effect, the response spectra of all 91 pulse-like motions were studied. Two normalizations were performed to facilitate comparison of the records. Rather than study the response spectra directly, deviations from predicted spectra were computed. These deviations are quantified by the parameter ε , which measures the number of standard deviations by which an observed spectral acceleration (Sa) differs from its predicted Sa at the given period

$$\varepsilon(T) = \frac{\ln Sa(T) - \mu_{\ln Sa(T)}}{\sigma_{\ln Sa(T)}} \quad (3)$$

where $\mu_{\ln Sa(T)}$ and $\sigma_{\ln Sa(T)}$ are the mean and standard deviation of a ground motion's log Sa value from a ground motion prediction model (e.g., Boore and Atkinson 2007), and $Sa(T)$ is the observed spectral acceleration value. The observation in Figure 4 that Sa 's are higher than predicted in the region of the pulse period means that we expect positive ε 's near T_p .

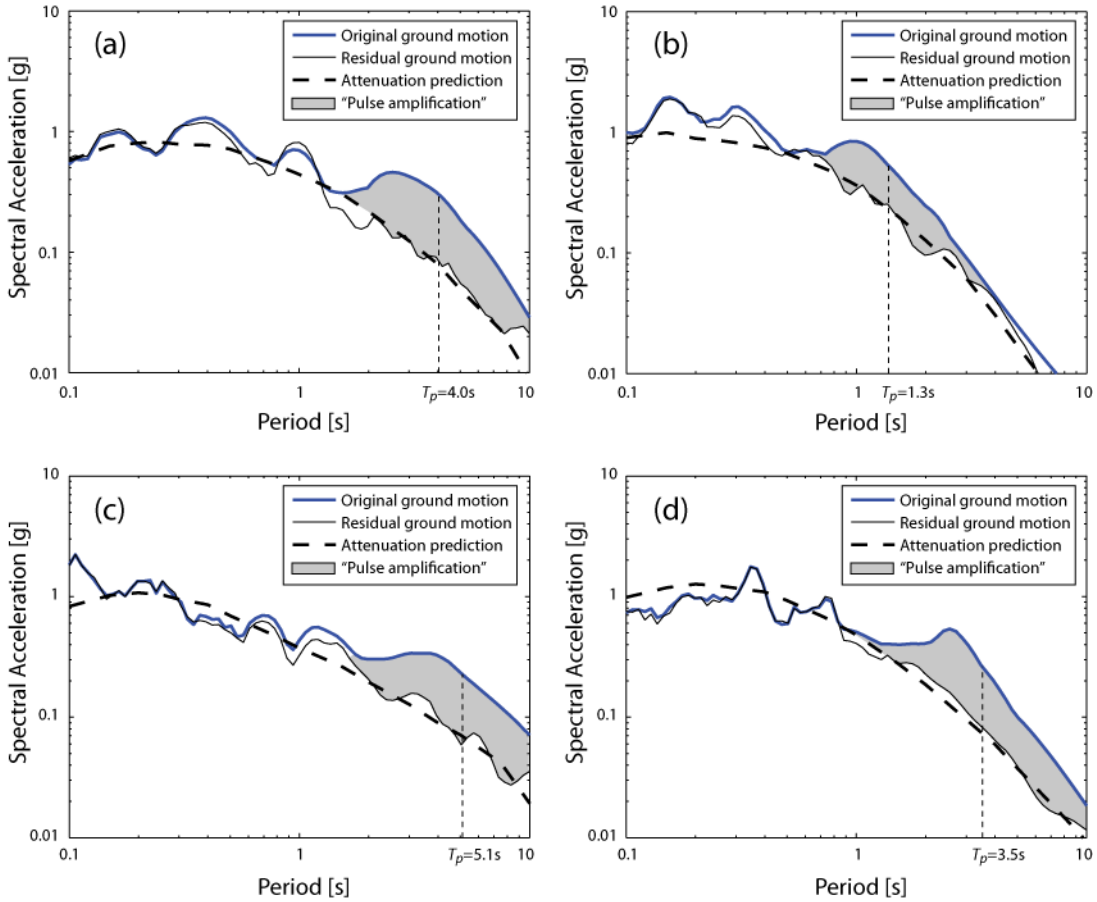


Figure 4: Response spectra of pulse-like ground motions before and after pulse extraction, and the Boore and Atkinson (2007) median prediction for each ground motion. (a) Imperial Valley, El Centro Array #5. (b) N. Palm Springs, N. Palm Springs. (c) Landers, Lucerne. (d) Northridge, Jensen Filter Plant Generator.

To allow comparison of records having differing pulse periods, we plot these ε 's versus T/T_p (where T_p is the period of the pulse), as shown in Figure 5a. It is clear from this figure that the response spectrum is systematically higher than predicted at $T = T_p$, with 90 of the 91 records having positive ε values, and the remaining record being only slightly negative. Next, in Figure 5b, we see the ε values of the residual ground motions (i.e., the ground motions with the pulses removed). The mean ε values

of these ground motions are very close to zero at all periods. This suggests that the residual ground motions have spectra that are on average equal to the predictive model, indicating that removal of the pulse did not overcompensate and make the residual records weaker than ground motion models would predict.

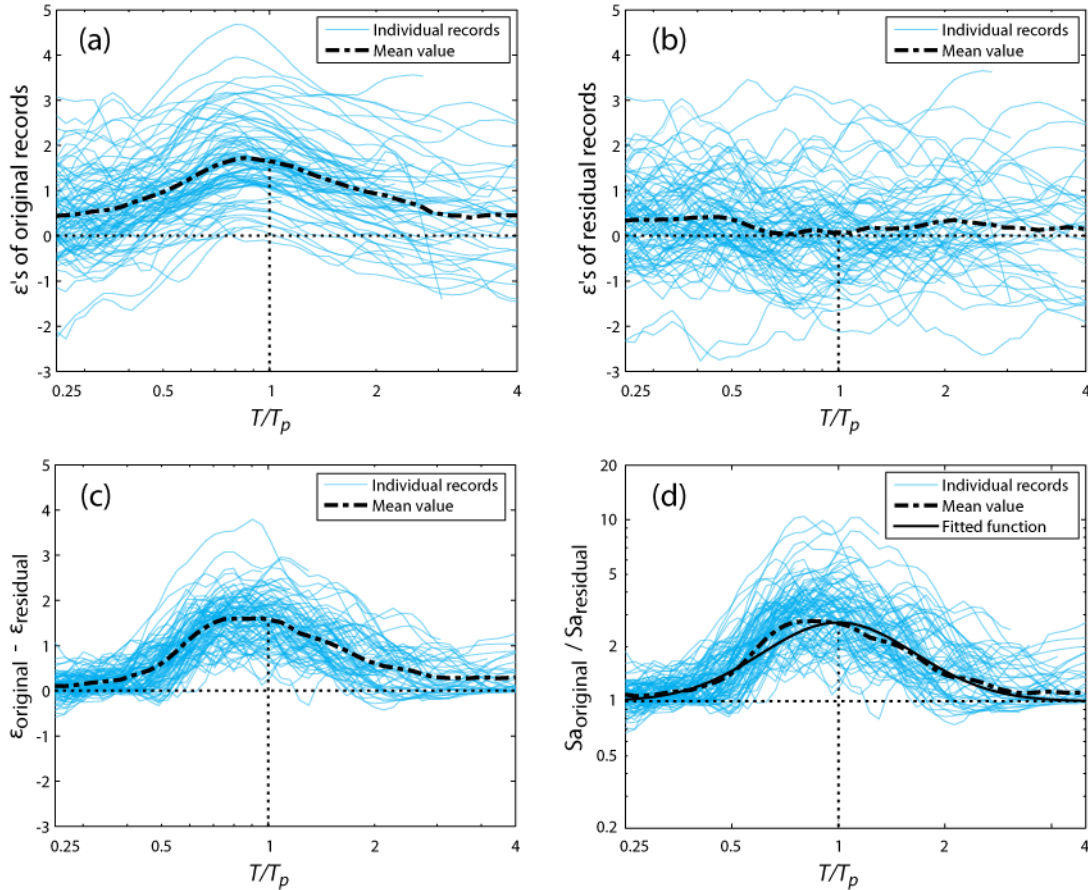


Figure 5: Epsilons and response spectra from pulse-like ground motions. (a) Epsilons from original ground motions. (b) Epsilons from residual ground motions. (c) Difference in ϵ between the original and residual ground motions. (d) Ratio of original spectral accelerations to residual spectral accelerations.

These results indicate that a practical approach to predict spectral accelerations of these records is to predict the spectra of the residual ground motions using existing ground motion models for “ordinary” motions, and then add an amplification factor around the pulse period to account for the contribution of the pulse. In Figure 5c, the difference in ϵ values between the original and residual ground motions is plotted. To make this result more conveniently usable in the form of a ground motion model, we return to spectral acceleration values in Figure 5d, where the ratios of the original record’s spectral acceleration value to the residual record’s spectral acceleration values are plotted. It is seen that addition of the pulse multiplies the spectral acceleration by an average of 2.7 at T_p , and 1.5 when $T/T_p = 2$ or 0.5. The mean value of this ratio is approximated by the following Gaussian (bell-curve) function around T_p

$$\ln \left[Sa_{original}(T) / Sa_{residual}(T) \right] = e^{-2\ln(T/T_p)} \quad (4)$$

This appears to closely fit the trend seen in Figure 5d, but future work will derive response spectra of the wavelet function used for pulse extraction, and may result in a more theoretically justified amplification function. This simple model, in which the amplification is only a function of pulse period, may also be refined after further study. It should be noted that Tothong (personal communication 2005, Tothong et al. 2007) was the first to develop and use a plot like Figure 5a, and the only new development here is to use wavelet processing to decouple Sa 's from the pulse and residual, so that they can be studied separately.

Given that the mean $\ln Sa$ of the residual ground motions is well-predicted by standard ground motion models (as seen in Figure 5b), and that the mean of the pulse amplification is well-predicted by equation (4), a simple ground motion model for pulse-like motions is given by:

$$\mu_{\ln Sa_{original}}(T, T_p) = \mu_{\ln Sa_{residual}}(T) + e^{-2\ln(T/T_p)} \quad (5)$$

where $\mu_{\ln Sa_{residual}}(T)$ is the mean logarithmic spectral acceleration value predicted by a standard ground motion model, and $\mu_{\ln Sa_{original}}(T, T_p)$ is the new prediction of the pulse-like ground motion. The standard deviation of normalized residuals from this prediction is approximately one, which indicates that the standard deviation of the original ground motion model need not be modified. Note that this prediction assumes the existence of a pulse, and also assumes knowledge of T_p (because the amplification function is dependent upon T_p). Because this model amplifies a narrow region around T_p rather than amplifying the response spectra in a more general way, it is classified as a “narrow-band” directivity model (Somerville 2003; Tothong et al. 2007).

IMPLICATIONS FOR SEISMIC HAZARD ANALYSIS

This model of the previous section can easily produce predicted response spectra for pulse-like motions with a given period, but not all near-fault records contain pulses, and pulses will also have varying periods. Probabilistic seismic hazard analysis accounts for unknown future magnitudes and distances when computing seismic hazard, and can be generalized to also account for unknown directivity effects in future ground motions. Tothong has described how these generalizations can be implemented, and presented the needed mathematics (Tothong et al. 2007). In addition to the response spectrum prediction presented here, and the prediction of pulse periods from equation (2), that procedure also requires a prediction of the probability that a pulse will occur at a given site susceptible to directivity; one such prediction is available from Iervolino and Cornell (2007). Calculations of this type, which explicitly account for directivity, can accurately amplify seismic hazard curves to account for pulses, and hazard deaggregation can also be used to identify the probability that a given ground motion intensity level is caused by a pulse-like ground motion. Further work is planned to more completely describe the orientation of velocity pulses, and that concept could also be adopted into a PSHA framework.

The focus of this work is on the impact of directivity pulses on response spectra, but the resulting structural responses may or may not be fully accounted for by the increased S_a values predicted here. Several researchers have concluded that S_a at the first-mode period of the structure is not sufficient to predict the effect of directivity pulses on nonlinear multi-degree-of-freedom structures (e.g., Alavi and Krawinkler 2001; Luco and Cornell 2007; Tothong and Cornell 2007 are recent examples among others). The S_a predictions presented here could also be incorporated into vector-valued PSHA, which Baker and Cornell found may account for directivity effects by measuring response spectra at multiple periods (2007). Further work is needed on this topic.

CONCLUSIONS

An algorithm for identifying strong velocity pulses in recorded ground motions has been briefly summarized and applied to a set of approximately 3500 fault-normal ground motions. The calculations identified 91 pulse-like ground motions and computed their associated pulse periods. Maps of these pulses suggest that many of them occurred at source-to-site geometries likely to have experienced directivity effects. The acceleration spectra of these 91 motions were then studied in more detail.

It was observed that the spectra of these records are systematically larger than predicted at periods near the velocity-pulse period. When the pulses were extracted from these records, the residual ground motions were well-described by existing ground motion prediction models, indicating that a simple narrow-band amplification could be applied around the pulse period to substantially account for the additional effect of the pulse. The 91 ground motions were used to estimate this amplification factor. The resulting prediction requires knowledge of the period of the pulse, which will not be known *a priori* for future ground motions. This can be addressed within probabilistic seismic hazard analysis, however, using the same approach by which uncertain future magnitudes and distances are currently addressed (Tothong et al. 2007). The resulting ground motion hazard curves should provide a more rigorous and justifiable accounting for the effects of directivity, and may provide tools to calibrate the near-fault design factors specified by building codes.

The large quantity of data used here is not easily reported in a written publication. A dedicated website has been created at <http://stanford.edu/~bakerjw/pulse-classification.html>, as a repository for algorithms, as well as a collection of figures showing time histories, response spectra and maps of this data. The website more completely documents the approach used here, and should be a useful resource for others interested in performing this type of analysis.

ACKNOWLEDGMENTS

Thanks to Polsak Tothong and Allin Cornell for discussions that motivated some of these calculations. This material is based upon work supported by the National Science Foundation under Award Number CMMI-0726684. Any opinions, findings, and conclusions or recommendations expressed in this publication are those of the author and do not necessarily reflect the views of the National Science Foundation.

REFERENCES

- Alavi, B., and Krawinkler, H. (2001). "Effects of near-fault ground motions on frame structures." *Blume Center Report #138*, Stanford, California, 301 p.
- Baker, J. W. (2007). "Quantitative Classification of Near-Fault Ground Motions Using Wavelet Analysis." *Bulletin of the Seismological Society of America*, 97(5), 1486-1501.
- Baker, J. W., and Cornell, C. A. (2007). "Vector-valued intensity measures for pulse-like near-fault ground motions." *Engineering structures*, (in press).
- Boore, D. M., and Atkinson, G. M. (2007). "Boore-Atkinson NGA Ground Motion Relations for Peak and Spectral Ground Motion Parameters." *PEER 2007/01*, Pacific Earthquake Engineering Research Center, Berkeley, California, 234 p.
- Bray, J. D., and Rodríguez-Marek, A. (2004). "Characterization of forward-directivity ground motions in the near-fault region." *Soil Dynamics and Earthquake Engineering*, 24(11), 815-828.
- Fu, Q., and Menun, C. (2004). "Seismic-environment-based simulation of near-fault ground motions." *Proceedings, 13th World Conference on Earthquake Engineering*, Vancouver, Canada, 15.
- Iervolino, I., and Cornell, C. A. (2007). "Prediction of the occurrence of velocity pulses in near-fault ground motions." *Bulletin of the Seismological Society of America*(in review).
- Luco, N., and Cornell, C. A. (2007). "Structure-Specific Scalar Intensity Measures for Near-Source and Ordinary Earthquake Ground Motions." *Earthquake Spectra*, 23(2), 357-392.
- Mallat, S. G. (1999). *A wavelet tour of signal processing*, Academic Press, San Diego.
- Mavroeidis, G. P., and Papageorgiou, A. S. (2003). "A Mathematical Representation of Near-Fault Ground Motions." *Bulletin of the Seismological Society of America*, 93(3), 1099-1131.
- Somerville, P. G. (2003). "Magnitude scaling of the near fault rupture directivity pulse." *Physics of the Earth and Planetary Interiors*, 137(1), 12.
- Somerville, P. G., Smith, N. F., Graves, R. W., and Abrahamson, N. A. (1997). "Modification of Empirical Strong Ground Motion Attenuation Relations to Include the Amplitude and Duration Effects of Rupture Directivity." *Seismological Research Letters*, 68(1), 199-222.
- Tothong, P., and Cornell, C. A. (2007). "Probabilistic Seismic Demand Analysis Using Advanced Ground Motion Intensity Measures, Attenuation Relationships, and Near-Fault Effects." *PEER 2006-10*, Pacific Earthquake Engineering Research Center, University of California at Berkeley, Berkeley, California, 205 p.
- Tothong, P., Cornell, C. A., and Baker, J. W. (2007). "Explicit-Directivity-Pulse Inclusion in Probabilistic Seismic Hazard Analysis." *Earthquake Spectra*, 23(4), 867-891